

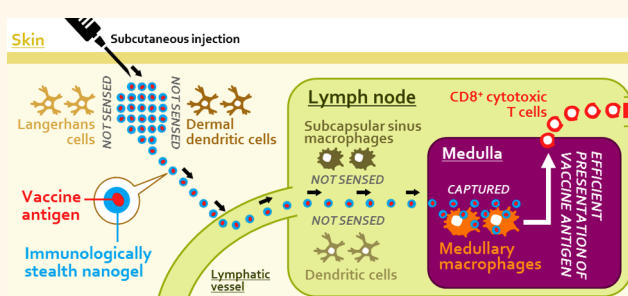
# Nanogel-Based Immunologically Stealth Vaccine Targets Macrophages in the Medulla of Lymph Node and Induces Potent Antitumor Immunity

Daisuke Muraoka,<sup>†,||</sup> Naozumi Harada,<sup>†,\*,||,\*</sup> Tae Hayashi,<sup>†</sup> Yoshiro Tahara,<sup>§,⊥</sup> Fumiyasu Momose,<sup>†</sup> Shin-ichi Sawada,<sup>§,⊥</sup> Sada-atsu Mukai,<sup>§,⊥</sup> Kazunari Akiyoshi,<sup>§,⊥</sup> and Hiroshi Shiku<sup>†,\*</sup>

<sup>†</sup>Department of Immuno-Geno Therapy, Mie University Graduate School of Medicine, Mie 514-8507, Japan, <sup>‡</sup>Basic and Preclinical Research, ImmunoFrontier, Inc., Tokyo 101-0021, Japan, <sup>§</sup>Department of Polymer Chemistry, Kyoto University Graduate School of Engineering, Kyoto 615-8510, Japan, and <sup>⊥</sup>ERATO, Japan Science and Technology Agency (JST), Tokyo 102-0076, Japan. <sup>||</sup>These authors contributed equally to this work.

**ABSTRACT** Because existing therapeutic cancer vaccines provide only a limited clinical benefit, a different vaccination strategy is necessary to improve vaccine efficacy. We developed a nanoparticulate cancer vaccine by encapsulating a synthetic long peptide antigen within an immunologically inert nanoparticulate hydrogel (nanogel) of cholesteryl pullulan (CHP). After subcutaneous injection to mice, the nanogel-based vaccine was efficiently transported to the draining lymph node, and was preferentially engulfed by medullary macrophages but was not sensed by other macrophages and dendritic cells (so-called “immunologically stealth mode”).

Although the function of medullary macrophages in T cell immunity has been unexplored so far, these macrophages effectively cross-primed the vaccine-specific CD8<sup>+</sup> T cells in the presence of a Toll-like receptor (TLR) agonist as an adjuvant. The nanogel-based vaccine significantly inhibited *in vivo* tumor growth in the prophylactic and therapeutic settings, compared to another vaccine formulation using a conventional delivery system, incomplete Freund's adjuvant. We also revealed that lymph node macrophages were highly responsive to TLR stimulation, which may underlie the potency of the macrophage-oriented, nanogel-based vaccine. These results indicate that targeting medullary macrophages using the immunologically stealth nanoparticulate delivery system is an effective vaccine strategy.



**KEYWORDS:** cancer vaccine · nanogel · vaccine delivery · macrophages · lymph node · T cells

Although immunotherapy is emerging as a new therapeutic modality for cancer, most of clinical trials of cancer vaccines have failed to prove their clinical activity thus far. A novel approach to improve immunogenicity and efficacy of cancer vaccines is therefore urgently needed. The primary target of vaccines is professional antigen-presenting cells (APCs) such as macrophages and dendritic cells (DCs), because these cells efficiently capture, process, and present vaccine antigens to both CD8<sup>+</sup> cytotoxic T cells and CD4<sup>+</sup> helper T cells in a major histocompatibility complex (MHC)-dependent manner. Simultaneously, professional APCs also provide T cells with co-stimulatory signals using a variety of membrane-bound proteins including CD80 and CD86.

Professional APCs thus control the quality, extent, and duration of T cell immunity. Vaccine delivery system targeting these professional APCs is therefore vital for the improvement of cancer vaccine efficacy. Recently, the use of synthetic nanoparticulate carriers has emerged as a novel strategy for effective vaccine delivery. When subcutaneously injected, nanoparticulate carriers preferentially enter into the lymphatic vessels, possibly prompted by interstitial fluid flow, and then move *via* lymphatic flow to the draining lymph node (DLN),<sup>1</sup> where various professional APCs survey and engulf particulate antigens by phagocytosis, macropinocytosis, and/or endocytosis, depending on the property of particles including size, surface charge, and presence of ligands for phagocyte

\* Address correspondence to nharada@clin.medic.mie-u.ac.jp, shiku@clin.medic.mie-u.ac.jp.

Received for review June 2, 2014 and accepted August 27, 2014.

Published online September 02, 2014  
10.1021/nn502975r

© 2014 American Chemical Society

surface receptors. *Via* this mechanism, nanoparticulate carriers are capable of successfully transporting antigens to professional APCs in the DLN<sup>1–3</sup> and enhance immunogenicity if applied to vaccines.<sup>4,5</sup>

In the efforts to exploit vaccine delivery for the improvement of efficacy, not macrophages but DCs have been considered as the most important target thus far, because antigen presentation by macrophages to T cells is thought to be less efficient than that by DCs.<sup>6</sup> However, in recent years, macrophages localized in lymph nodes are beginning to attract interest, because a recent finding indicates a specific subset of lymph node macrophages also may play a major role as APCs in tumor vaccination; subcutaneously injected dead tumor cells containing particulate antigens induce antigen-specific CD8<sup>+</sup> T cell response dependent on CD169<sup>+</sup> macrophages in the DLN but not on migratory DCs or lymph node-resident conventional DCs.<sup>7</sup> Another study also shows that lymph node macrophages as well as DCs play a significant role in cross-presentation of subcutaneously injected, microsphere-encapsulated antigen.<sup>8</sup> Thus, certain population(s) of lymph node macrophages might have a remarkable cross-presenting activity and might serve as a preferential target for vaccines. However, no delivery system selective for these macrophages has been available, and the usefulness of these cells in vaccination has been unexplored.

We have developed a series of nanosized hydrogel particles (nanogels) to create novel nanomaterials for biomedical applications.<sup>9</sup> In particular, cholesteryl pullulan (CHP), a pullulan polysaccharide partially hydrophobized by a chemical modification with cholesteryl groups, forms physically cross-linked nanogel particles with a diameter of ~50 nm *via* self-assembly in water.<sup>10,11</sup> CHP efficiently forms a stable complex with a polypeptide through hydrophobic interactions<sup>12</sup> and thereby helps solubilization and long-term stabilization of the polypeptide. Fabrication of the CHP:polypeptide complex is feasible, simple, and reproducible. These features of the CHP nanogel make it an ideal nanoparticulate carrier for the delivery of polypeptide-based therapeutic molecules.<sup>13,14</sup> Besides, when used for *in vitro* antigen delivery, the CHP nanogel enhances cross-presentation of protein antigen.<sup>15,16</sup> This finding led us to evaluate the CHP nanogel as a vaccine delivery system in a series of clinical studies.<sup>17</sup> However, the behavior of CHP nanogel *in vivo* has been unclear so far. In the present study, we investigated *in vivo* vaccine delivery function of the CHP nanogel in detail. When subcutaneously injected, the CHP nanogel efficiently travels to the DLN owing to its small size and uncharged surface. The CHP nanogel is immunologically inert (*i.e.*, the lack of either potential ligands for or stimulatory activity toward immune cells); hence, it evades capture by immune cells including DCs in the DLN. The CHP nanogel then reaches the medulla,

a central area of lymph node, where it is vastly engulfed by medullary macrophages. We termed such behavior of the CHP nanogel “immunologically stealth mode”. Although the function of medullary macrophages has so far remained elusive, the CHP nanogel-based vaccine elicits a strong antitumor T cell response dependent on these cells. Thus, we simultaneously identified medullary macrophages as a useful cancer vaccine target and the CHP nanogel as a novel delivery system specific for these cells, providing a new strategy to enhance vaccine efficacy.

## RESULTS

### Immunologically Inert CHP Nanogel Is Selectively Engulfed by Medullary Macrophages in the Lymph Node.

CHP was synthesized by grafting 0.9–1.5 cholesterol groups to every 100 glucose units on a hydrophilic pullulan polysaccharide (mean molecular weight 100 000) (Figure 1a). In water, CHP spontaneously forms an uncharged nanogel with a diameter of 40–60 nm *via* hydrophobic interaction among cholesterol groups (Figure 1b and Table 1).<sup>10,11</sup> We supposed that the CHP nanogel may efficiently travel to the DLN when subcutaneously injected, because the nanogel is small enough (<100 nm) to pass through the clefts and pores of lymphatic vessels and its uncharged hydrophilic surface would prevent nonspecific binding to the extracellular matrix and cells. Indeed, the CHP nanogel accumulated in the DLN after subcutaneous administration to mice (Figure 1c). Previous works demonstrated that a potential receptor for pullulan, the backbone of CHP, is not detected in the lymphoid tissues,<sup>18,19</sup> indicating that immune cells in lymph nodes do not express the receptor. In addition, the CHP nanogel possesses no stimulatory activity toward macrophages and DCs (Supporting Information, Figure S1). These facts indicate that the CHP nanogel has neither affinity for nor effect on immune cells, *i.e.*, it is immunologically inert. We therefore anticipated that lymph node cells do not engulf the CHP nanogel, and indeed, uptake by DCs (CD11c<sup>+</sup>F4/80<sup>-</sup>), B cells (CD45R/B220<sup>+</sup>), or T cells (CD3e<sup>+</sup>) was quite low or absent (Figure 1d). However, intriguingly, massive accumulation was observed in macrophages (F4/80<sup>+</sup>CD11b<sup>+</sup>). This result led us to examine the ability of the CHP nanogel to deliver a vaccine antigen selectively to lymph node macrophages. We prepared a complex of the CHP nanogel with a chemically synthesized long peptide antigen (LPA) (the CHP:LPA complex; Table 1, Figure 2a, and Supporting Information, Figure S2). LPA was designed to include an epitope recognized by mouse CD8<sup>+</sup> cytotoxic T cells, *i.e.*, the epitope derived from either a murine tumor-specific antigen mutated ERK2 (mERK2)<sup>20</sup> or a clinically relevant human tumor antigen MAGE-A4.<sup>21</sup> When the CHP:LPA complex was exposed to serum *in vitro*, the LPA still existed as the complex (more than 20% of LPA at least) over 40 h (Supporting

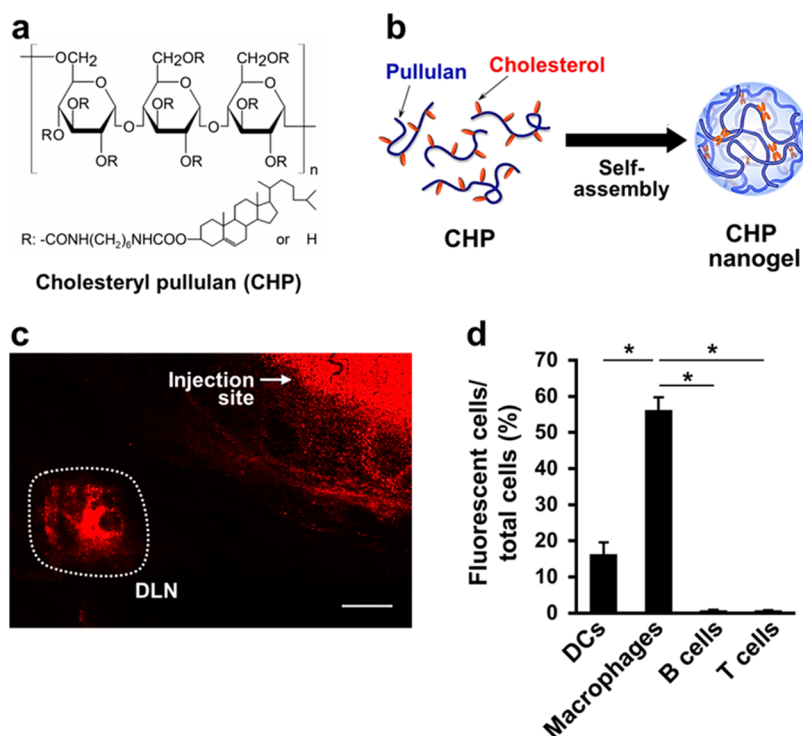


**Figure 1.** The CHP nanogel is selectively incorporated into macrophages in the DLN after subcutaneous injection to BALB/c mice. (a) Chemical structure of CHP. (b) Schematic representation of nanogel formation *via* self-assembly of CHP. CHP forms a nanogel by hydrophobic interaction between cholesteryl groups in an aqueous solution. (c) *In situ* confocal laser scanning microscopy analysis of a DLN of a mouse that received subcutaneous injection of the rhodamine-labeled CHP nanogel. The scale bar is 1 mm. (d) Incorporation of the subcutaneously injected rhodamine-CHP nanogel (0.5 mg) into immune cells in the DLN of BALB/c mice (three mice per group). Sixteen hours after the injection, uptake of the rhodamine-CHP nanogel was evaluated using flow cytometry in DCs ( $CD11c^+F4/80^-$ ), macrophages ( $F4/80^+CD11b^+$ ), B cells ( $CD45R/B220^+$ ), and T cells ( $CD3\epsilon^+$ ) isolated from the DLN. Data are mean  $\pm$  SD; *p*-values were determined by Dunnett's multiple comparison test. \**p* < 0.05. Experiments were performed in triplicate.

**TABLE 1. Dynamic Light Scattering Analysis and  $\zeta$ -Potential Measurement of the Nanogels or the Complex between CHP<sup>a</sup> Nanogel and LPA<sup>b</sup>**

nanogel or CHP:LPA complex	amino acid sequence of LPA <sup>c</sup>	size (d, nm)	$\zeta$ -potential (mV)
CHP	None	42	-4.6
CHP-NH <sub>2</sub>	None	86	16.1
CHG <sup>d</sup>	None	183	-1.9
CHP:mERK2 LPA	NDHIAYFLYQILRGLQYIHSANVLHRDLKPSNLLNT	57	-2.7
CHP:MAGE-A4 LPA	GSNPARYEFLWGPRLAETSYYKVLHVVVRVNRVRIAYP	57	-3.0

<sup>a</sup> Cholesteryl pullulan. <sup>b</sup> Long peptide antigen. <sup>c</sup> Underline indicates the epitope recognized by mouse CD8<sup>+</sup> cytotoxic T cells. <sup>d</sup> Cholesteryl glycogen.

Information, Figure S3). After subcutaneous injection into mice, the CHP:mERK2 LPA complex was largely captured by macrophages but not by other immune cells including DCs in the DLN (Figure 2b). The CHP:MAGE-A4 LPA complex also gave a similar result (data not shown). The mERK2 LPA complexed with a cationic (CHP-NH<sub>2</sub>) or large-sized (cholesteryl glycogen, CHG; >100 nm) nanogel was not detected in the organ (Table 1 and Figure 2c), indicating that the size and surface charge of nanoparticle is critical for its transportation to lymph node. Further dissection of the macrophage subsets<sup>22</sup> incorporating the CHP:mERK2 LPA revealed that the uptake occurred in medullary sinus macrophages (MSMs,  $F4/80^+CD169^+$ ) and medullary cord macrophages (MCMs,  $F4/80^+CD169^-$ ), but

not in subcapsular sinus macrophages (SSMs,  $F4/80^-CD169^+$ ) (Figure 2d,e). A similar result was also obtained with the CHP:MAGE-A4 LPA (data not shown). Histochemical analysis of the DLN showed that the cells incorporating the complex of CHP and fluorescently labeled LPA had a large and round shape and were located in the medullary region of the lymph node (Supporting Information, Figure S4), thus showing characteristics of medullary macrophages. According to these data, we identified the CHP nanogel as a novel nanomaterial suitable for selective vaccine delivery to medullary macrophages in lymph nodes.

**LPA Delivered by the CHP Nanogel Is Cross-Presented by Medullary Macrophages to CD8<sup>+</sup> Cytotoxic T Cells with High Efficiency.** The CHP nanogel allows us to deliver

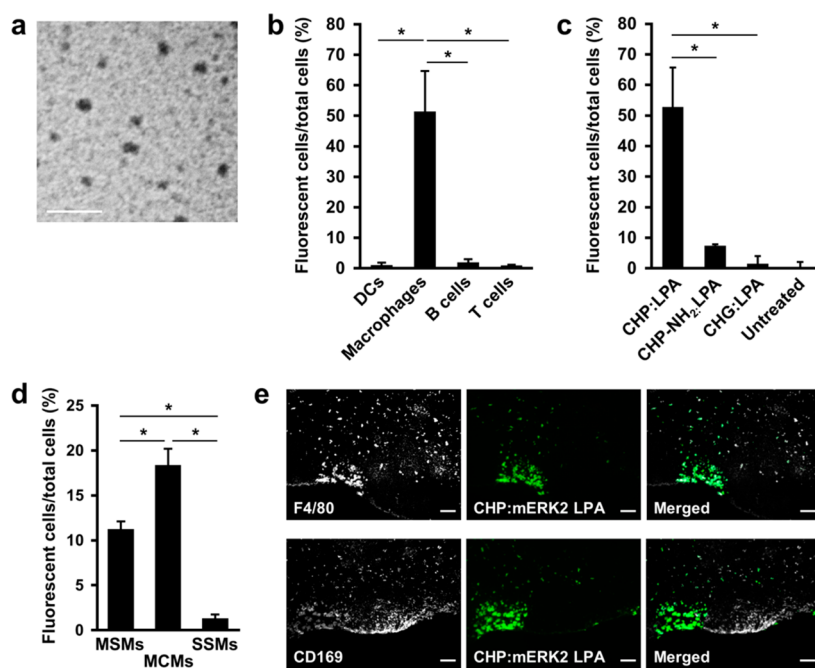


**Figure 2.** The CHP nanogel:LPA complex is selectively and efficiently engulfed by medullary macrophages in the DLN after subcutaneous injection to BALB/c mice. (a) Transmission electron microscopy of the CHP:LPA complex. The scale bar is 100 nm. (b) Uptake of the CHP:FAM-labeled mERK2 LPA complex in immune cells in the DLN. (c) Uptake of the complexes of indicated nanogels and FAM-mERK2 LPA in macrophages in the DLN. (d) Uptake of the CHP:FAM-mERK2 LPA complex in MSMs ( $F4/80^+CD169^+$ ), MCMs ( $F4/80^+CD169^-$ ), and SSMs ( $F4/80^-CD169^+$ ) in the DLN. (e) Immunohistochemical analysis of incorporation of the CHP:FAM-mERK2 LPA into medullary macrophages. The scale bar is 100  $\mu\text{m}$ . The experiments in panels b–d were performed as in panel d of Figure 1 using the complexes of nanogel and FAM-mERK2 LPA (50  $\mu\text{g}$ ). Data are mean  $\pm$  SD of triplicates. *p*-values were determined by Dunnett's multiple comparison test. \**p* < 0.05. The experiments were repeated thrice with similar results.

a vaccine antigen to medullary macrophages selectively, but the ability of these macrophages to stimulate antigen-specific  $CD8^+$  T cells and their usefulness as a vaccine target have not been studied to date. Therefore, we tested whether these macrophages cross-present a vaccine antigen in mice injected with the CHP:mERK2 LPA and a Toll-like receptor (TLR) 9 agonist, CpG oligodeoxynucleotide (CpG ODN), as an adjuvant.<sup>23,24</sup> Whole lymph node cells isolated from the DLN of the mice effectively stimulated DUC18  $CD8^+$  T cells that express a transgene of T cell receptor (TCR) recognizing a mERK2-derived, tumor-specific epitope<sup>25</sup> within the mERK2 LPA (Figure 3a). This stimulation occurred only in the presence of CpG ODN. Macrophages ( $F4/80^+CD11b^+$ ) purified from whole lymph node cells also cross-presented the antigen, whereas the macrophage-negative fraction ( $F4/80^-CD11b^-$ ) lacked such activity and DCs ( $CD11c^+F4/80^-$ ) were evidently inferior to macrophages in our system (Figure 3b,c), in agreement with the uptake of CHP:LPA to these cell populations (Figure 2b). To identify the subset of macrophages responsible for this cross-presentation, we purified MSMs ( $F4/80^+CD169^+$ ) and MCMs ( $F4/80^+CD169^-$ ) from the immunized mice (Supporting Information, Figure S5). MSMs and MCMs both competently cross-presented the vaccine antigen to DUC18  $CD8^+$  T cells (Figure 3d,e).

The activity of MSMs was higher than that of MCMs, indicating that MSM is the cell type most capable of cross-presenting antigens. Subcutaneous injection of a liposomal formulation of clodronate (clodronate liposome) into mice selectively depleted macrophages but not DCs in lymph nodes (Supporting Information, Figure S6).<sup>8,26</sup> After ablation by clodronate liposomes of lymph node macrophages, *in vivo* induction of the LPA-specific  $CD8^+$  T cell response was significantly impaired (Figure 3f). Taken together, these data support the notion that medullary macrophages in lymph nodes can effectively cross-prime  $CD8^+$  T cells.

**Vaccination with the CHP Nanogel:LPA Complex and TLR Agonist as Adjuvant Elicits Vaccine-Specific, Strong  $CD8^+$  T Response and Effectively Suppresses *In Vivo* Tumor Growth.** On the basis of the finding that the CHP nanogel vaccine selectively targets medullary macrophages possessing high cross-presenting activity, we expected that this vaccine system could induce a potent antitumor  $CD8^+$  T cell response. We next evaluated antitumor efficacy of the CHP:LPA complex vaccine in a mouse pharmacological model compared to that of a vaccine containing LPA emulsified in incomplete Freund's adjuvant (IFA), a widely used conventional vaccine delivery system that is known to exert the depot effect at the injection site. The immune response induced by an IFA-based vaccine is reported to be mediated by DCs.<sup>27</sup>

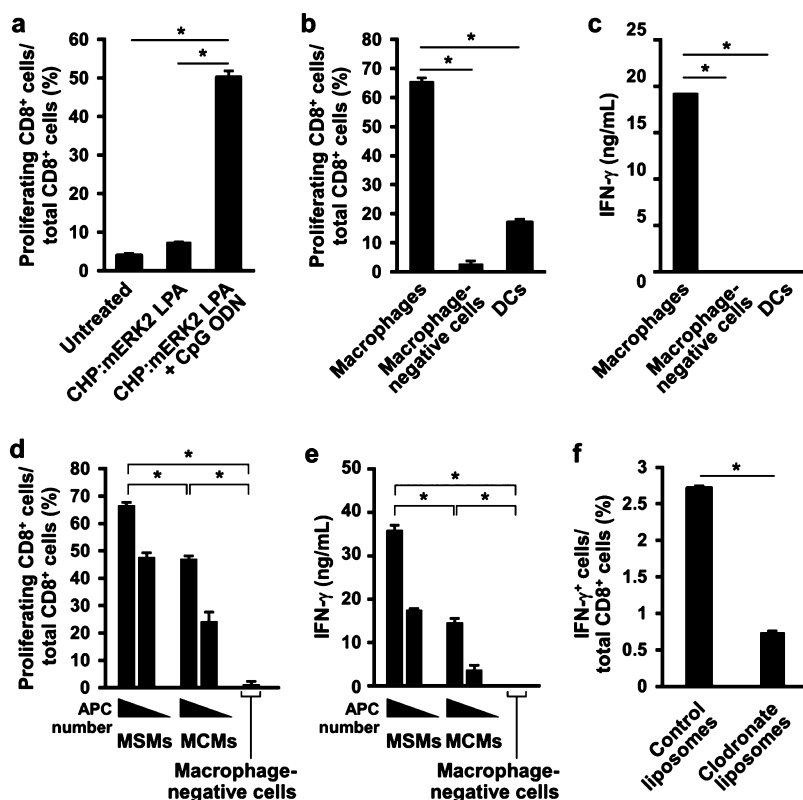


**Figure 3.** Medullary macrophages directly and efficiently cross-present antigens to specific CD8<sup>+</sup> T cells. (a–e) The CHP:mERK2 LPA complex with or without CpG ODN was injected into the footpad of BALB/c mice. Eighteen hours later, the whole lymph node cells (a) or the fractions containing macrophages (F4/80<sup>+</sup>CD11b<sup>+</sup>), macrophage-negative cells (F4/80<sup>+</sup>CD11b<sup>-</sup>), and DCs (CD11c<sup>+</sup>F4/80<sup>-</sup>) (panels b and c) were isolated from the DLN. Macrophages were further separated into MSMs (CD169<sup>+</sup>) and MCMs (CD169<sup>-</sup>) (panels d and e, for the gating strategy in cell sorting, see Supporting Information, Figure S5). These cells were cocultured as APCs with mERK2-specific DUC18 CD8<sup>+</sup> T cells for 48 h *in vitro*. (a, b, and d) Proliferation of DUC18 CD8<sup>+</sup> T cells was measured using a CFSE dilution assay. The numbers shown in histograms indicate the percentages of proliferating cells. (c and e) The concentration of IFN- $\gamma$  produced by CD8<sup>+</sup> T cells into the culture supernatant was determined using ELISA. (f) Clodronate liposomes or control liposomes were subcutaneously injected into the footpad of BALB/c mice, and 6 days later, the CHP:mERK2 LPA was injected at the same site. Seven days after the immunization, splenocytes were isolated and restimulated with mERK2 LPA *in vitro*. Activated specific CD8<sup>+</sup> T cells were quantified using intracellular IFN- $\gamma$  staining followed by flow cytometry (two mice per group). The data are mean  $\pm$  SD of triplicates. *p*-values were determined using Tukey-Kramer multiple comparison test, Dunnett's multiple comparison test, and Student's *t* test in panels a, d, and e; panels b and c; and panel f, respectively. \**p* < 0.05. The results are representative of one of at least two experiments.

We also observed that the IFA:LPA vaccine is dependent on DCs but not on macrophages (Supporting Information, Figure S7). Using these two vaccine delivery systems, we evaluated the inhibitory effect of vaccination with the mERK2 or MAGE-A4 LPA on tumor growth in mice transplanted with syngeneic tumors. Tumors included murine fibrosarcoma CMS5a cells<sup>28,29</sup> expressing endogenous mERK2 and murine colon carcinoma CT26 cells<sup>30</sup> stably expressing a transgene of human MAGE-A4 (CT26/MAGE-A4).<sup>21</sup> As a result, in the prophylactic setting, growth of both types of tumors was significantly inhibited in the mice vaccinated with the CHP:LPA complex relative to the control group (Figure 4a,b). Vaccination with the IFA:LPA was almost ineffective against the CMS5a tumor, and was less effective than vaccination with the CHP:LPA against the CT26/MAGE-A4 tumor. All of mice rejected the CT26/MAGE-A4 tumor in the CHP:LPA vaccine group (*n* = 7), while only one animal did in the IFA:LPA vaccine group (*n* = 7) (Figure 4b). Efficacy of the

vaccines was also evaluated in the therapeutic setting; vaccination with the CHP:MAGE-A4 LPA and CpG ODN significantly suppressed the growth of CT26/MAGE-A4 tumor, while the IFA:LPA vaccine and CpG ODN or CpG ODN alone did not affect the tumor growth (Figure 4c). The ability of the CHP:LPA and IFA:LPA vaccines to induce antigen-specific CD8<sup>+</sup> T cell response was also assessed by immunizing mice in a manner similar to the tumor development experiment above. Seven days after the last vaccination, the frequency of LPA-specific CD8<sup>+</sup> T cells in the spleen was measured (Figure 4d,e). The CHP:LPA and IFA:LPA vaccines both induced a measurable specific CD8<sup>+</sup> T cell response when administered with TLR agonists such as a TLR9 agonist CpG ODN or a TLR3 agonist poly-ICLC RNA, but not in the absence of TLR stimulation. Notably, in accordance with the *in vivo* tumor growth experiment, the frequency of specific CD8<sup>+</sup> T cells was much higher in mice immunized with the CHP:LPA than in those immunized with the IFA:LPA. This result indicated that



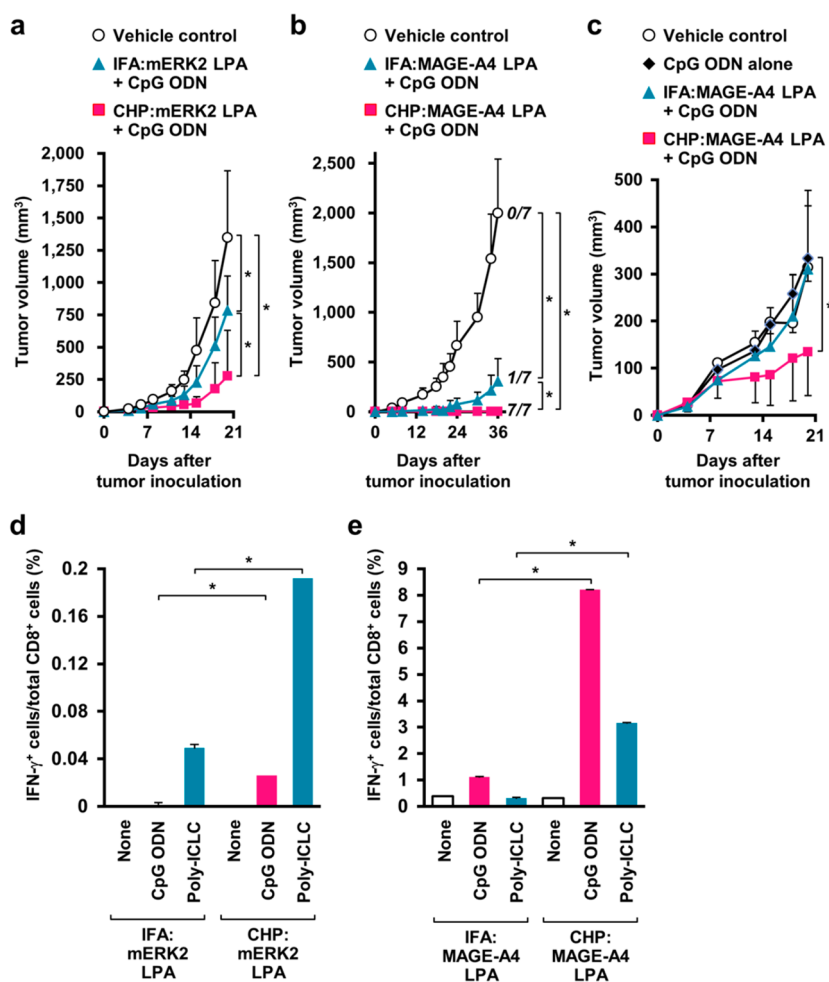


**Figure 4.** The macrophage-selective nanogel-based vaccine shows strong antitumor efficacy and CD8<sup>+</sup> T cell-inducing activity in the presence of Toll-like receptor TLR agonists as an adjuvant. (a and b) Effects of vaccination on *in vivo* tumor growth in the prophylactic setting. The LPA (50  $\mu$ g) complexed with either CHP nanogel or IFA was subcutaneously injected into BALB/c mice followed by immediate injection of CpG ODN (50  $\mu$ g) on day -7. On day 0, 10<sup>6</sup> CM55a cells (a) or CT26/MAGE-A4 cells (b) were subcutaneously transplanted into the mice. Subsequently, the tumor volume was measured three times a week. Numbers in italic in panel b indicate the mice who rejected the tumor. Each group included 4–7 mice. (c) Effects of vaccination on *in vivo* tumor growth in the therapeutic setting. This experiment was performed in a way similar to panel b, but the vaccines were administered at days 4 and 11 and the dose of CpG ODN was 25  $\mu$ g. (d and e) Antigen-specific CD8<sup>+</sup> T cell response induced by the vaccines. BALB/c mice were injected with either the CHP:LPA or IFA:LPA vaccine. Some groups were also injected with CpG ODN (50  $\mu$ g) or poly-ICLC RNA (50  $\mu$ g) immediately after administration of vaccine. Seven days after vaccination, splenocytes were isolated and restimulated with mERK2 LPA or MAGE-A4 LPA *in vitro*. Frequency of activated specific CD8<sup>+</sup> T cells was quantified by intracellular IFN- $\gamma$  staining followed by flow cytometry (two mice per group). The data are mean  $\pm$  SD. *p*-values were determined by Student's *t* test. \**p* < 0.05. These experiments were repeated at least twice with similar results.

TLR agonists had a greater adjuvant effect on the CHP:LPA vaccine than on the IFA:LPA vaccine. We also confirmed that the CHP:LPA vaccine elicited a much greater CD8<sup>+</sup> T cell response when compared to a saline-based vaccine (Supporting Information, Figure S8). Altogether, these data demonstrate that the lymph node macrophage-targeted nanogel-based vaccine system showed a remarkable antitumor effect through enhanced induction of tumor-specific CD8<sup>+</sup> T cells.

**Lymph Node Macrophages Are Highly Sensitive to TLR Stimulation: A Possible Mechanism for the Potency of CHP nanogel-Based Vaccine.** Lymph node macrophages efficiently cross-presented nanoparticulate antigen delivered by the CHP nanogel, but only in the presence of

TLR stimulation. By analyzing the susceptibility of lymph node macrophages to TLR stimulation, we investigated a possible mechanism that underlies the observed strong cross-presenting activity. Incorporation of subcutaneously injected, fluorescently labeled CpG ODN into macrophages (F4/80<sup>+</sup>CD11b<sup>+</sup>) and DCs (CD11c<sup>+</sup>F4/80<sup>-</sup>) in the DLN was assessed in mice. Higher accumulation of CpG ODN was observed in macrophages than in DCs (Figure 5a). Uptake of another TLR agonist, poly-ICLC RNA, could not be examined because of the lack of an appropriate analytical method. Activation of macrophages and DCs in the DLN by CpG ODN or poly-ICLC RNA was then determined based on the expression of co-stimulatory

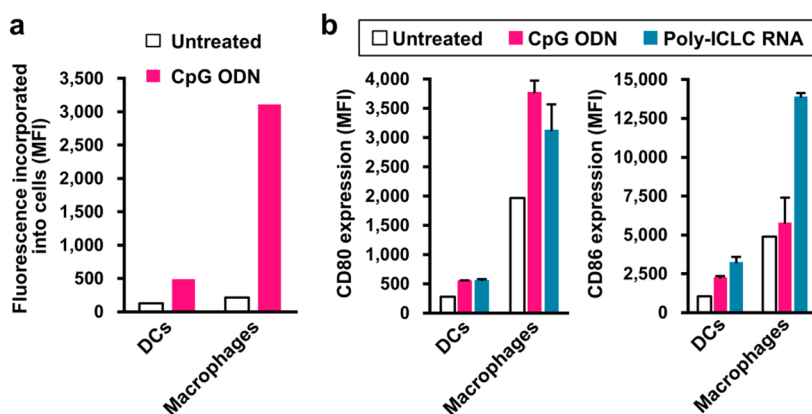


**Figure 5.** Lymph node macrophages are highly responsive to TLR agonists. (a) Incorporation of subcutaneously injected, FITC-labeled CpG ODN into macrophages and DCs in the DLN. BALB/c mice (two mice per group) were injected with FITC-CpG ODN (50  $\mu$ g), and 16 h later, macrophages (F4/80<sup>+</sup>CD11b<sup>+</sup>) and DCs (CD11c<sup>+</sup>F4/80<sup>-</sup>) in the DLN were isolated, and uptake of FITC-CpG ODN in these cells was measured using flow cytometry. (b) Activation of macrophages and DCs in the DLN by TLR agonists. BALB/c mice (two mice per group) were subcutaneously injected with CpG ODN (50  $\mu$ g) or poly-ICLC RNA (50  $\mu$ g), and 16 h later, macrophages and DCs in the DLN were tested for expression of CD80 and CD86. MFI, mean fluorescence intensity.

molecules CD80 and CD86. In accordance with the uptake of CpG ODN, the up-regulation of CD80 and CD86 by TLR stimulation was prominent in macrophages (Figure 5b). These data revealed that lymph node macrophages are highly responsive to TLR stimulation, and possibly this way they acquire the high cross-presenting activity. Therefore, concurrent, appropriate TLR stimulation would be a prerequisite for the activity of macrophage-dependent CHP nanogel-based vaccine. Conversely, thanks to the high susceptibility of lymph node macrophages to TLR stimulation, the CHP nanogel-based vaccine would acquire its high potency.

## DISCUSSION

Thus far, no antigen delivery system targeting macrophages localized in the lymph node has been available, although several vaccine formulations selective for splenic macrophages have been developed including a microparticulate antigen with a diameter of 0.5  $\mu$ m for MARCO<sup>+</sup> macrophages<sup>31</sup> and an anti-CD169 antibody-fused protein antigen for CD169<sup>+</sup> macrophages.<sup>32</sup> The present study showed for the first time that the CHP nanogel functions as a lymph node medullary macrophage-selective vaccine delivery system. A precise mechanism for the preferential incorporation of the CHP nanogel into medullary macrophages has yet to be elucidated, but the unique characteristics of CHP nanogel may help to explain that phenomenon. Because the CHP nanogel is immunologically inert, immune cells including DCs would not be able to sense and engulf the nanogel. Nevertheless, medullary macrophages can, likely due to their very high phagocytic activity.<sup>22</sup> Thus, the CHP nanogel-based vaccine likely acquires its macrophage-selective delivery function as a consequence of avoiding surveillance by other cells (the “immunologically

stealth vaccine”). The difference between medullary and subcapsular sinus macrophages also may be explained by a similar reason.<sup>22</sup> The present study also validated a novel approach to give a material a delivery function targeting a certain immune cell population by strictly preventing acquisition by unintended cells.

The functions of medullary macrophages that involve scavenging of pathogens and particulate antigens from the lymph and supporting plasma-cell survival have been reported,<sup>22</sup> but their involvement in the induction of T cell response has been unexplored. To our knowledge, the present study is the first report describing the participation of medullary macrophages in T cell immunity. Cross-presentation by these macrophages required the presence of TLR agonist probably because the TLR stimulation up-regulated the phagocytic, antigen processing, and/or presenting functions of these macrophages. On the other hand, it is also possible that TLR stimulation attenuates cross-presentation, because TLR stimulation is also known to increase the digestive activity of phagosomes that destroys antigens,<sup>33</sup> which can result in destruction of putative epitopes. Medullary macrophages may possess some intrinsic mechanism to avoid this effect, for example, increased escape of antigens from phagosomes to the cytosol.<sup>34</sup> Alternatively, the CHP nanogel may protect antigens from excess degradation in phagosomes. We also confirmed that similar to murine macrophages, human macrophages were also highly capable of cross-presenting antigens but only in the presence of TLR stimulation (Supporting Information, Figure S9). To further evaluate the significance of cross-presentation by lymph node macrophages and to harness it for effective tumor vaccination, the direct and/or indirect mechanisms by which TLR stimulation regulates the quality

and outcome of macrophage-mediated cross-presentation should be clarified in the future.

## CONCLUSION

The present study demonstrated that selective vaccine delivery to medullary macrophages localized in the medulla, the core of lymph nodes, can be achieved by using an immunologically stealth nanoparticulate delivery system. We also revealed that medullary macrophages have a potential to effectively induce specific CD8<sup>+</sup> T cell response to vaccines. These two key findings build a theoretical basis to design a

macrophage-oriented cancer vaccine with high potency, which may overcome the limited clinical efficacy of existing cancer vaccines. This strategy may improve the therapeutic efficacy of vaccines against not only cancers but also infectious diseases reactive to T cell immunity, and may thus have great impact in the field of immunotherapy. Cancer vaccines utilizing the CHP nanogel used in the present study have already been tested in clinical trials and confirmed to be highly safe and immunogenic, also supporting the clinical application of macrophage-oriented vaccines utilizing this nanoparticulate delivery system.

## MATERIALS AND METHODS

**Fabrication and Analysis of the Complex of CHP Nanogel with LPA.** CHP, rhodamine-labeled CHP, CHP-NH<sub>2</sub>, and CHG were synthesized as described previously.<sup>35–37</sup> LPAs were chemically synthesized by Bio-Synthesis, Inc. (Lewisville, TX). The sequences of the LPAs used were as follows: human MAGE-A4-derived LPA (GSNPARYEFLWGPRALAEYSVYKLEHVVRVNRVRIAYP), mERK2-derived LPA (NDHIAYFLYQILRGLQYIHSANVLRDLKPSNLLNT), and human NMW LPA (SLLMWITQCYYYYYYNYKRCFPVYYYYYYCMTWNQMNL). The MAGE-A4 LPA and mERK2 LPA contain epitopes for murine CD8<sup>+</sup> T cells (underlined), and the human NMW LPA does for HLA-A2-restricted NY-ESO-1, HLA-A24-restricted MAGE-A4, and HLA-A24-restricted WT1 epitopes (bold). For analysis of antigen incorporation, these LPAs were labeled with fluorescein amidite (FAM). LPA and CHP were dissolved in dimethyl sulfoxide and phosphate-buffered saline (PBS) containing 6 M urea, respectively. Both solutions were combined and gently mixed at room temperature, followed by dialysis against PBS to remove urea. The resulting solution of the CHP:LPA complex was stored at 4 °C until use. The peptide concentration in the CHP:LPA complex solution was determined by measuring the absorbance at 280 nm, where CHP does not contribute to absorbance. The final concentration of CHP was approximately 10 mg/mL and that of LPA was 0.2–0.4 mg/mL. Complexation of the CHP nanogel and FAM-labeled LPA was confirmed by means of high performance size exclusion chromatography (HPSEC) using a Superose 12 10/300 GL column (GE Healthcare). An aliquot of the sample was injected into the HPSEC system (Shimadzu), eluted with PBS, and detected by means of ultraviolet absorbance at 495 nm. To determine the size of the CHP nanogel and CHP:LPA complex, dynamic light scattering measurement was performed using a Zetasizer Nano ZS (Malvern Instruments, Ltd.) at 633 nm and a 173° detection angle at 25 °C. The measured autocorrelation function was analyzed using the cumulant method. The hydrodynamic diameter ( $D_h$ ) of the samples was calculated from the Stokes–Einstein equation. The  $\zeta$ -potential of CHP:LPA complex was also measured using the Zetasizer Nano ZS at a 90° detection angle at 25 °C in PBS. The mERK2 CHP:LPA complex was also analyzed using transmission electron microscopy (TEM). Briefly, the sample was applied to a carbon-coated grid, and the grid was stained with TI blue (Nissin EM, Japan), dried, and subjected to TEM (HT7700, Hitachi) at an accelerating voltage of 100 kV.

**Mice and Tumors.** Female BALB/c mice were obtained from SLC Japan and used at 6–12 weeks of age. DUC18 mice, transgenic for TCR $\alpha/\beta$  that interacts with a K<sup>d</sup>-restricted mERK2<sub>136–144</sub> peptide epitope, were established as described previously.<sup>25</sup> CD90.1-congenic BALB/c mice were kindly provided by Dr. Sakaguchi of Osaka University, Japan. We mated DUC18 mice and CD90.1-congenic mice at our animal facility, and obtained DUC18/CD90.1 mice. T cells isolated from these mice can be traced in *in vitro* and *in vivo* experiments using anti-CD90.1 antibody. All mice were maintained at the Experimental Animal Facility of Mie University. The experimental protocol was

approved by the Ethics Review Committee for Animal Experimentation of Mie University.

CT26 is a colon epithelial tumor cell line that was produced by intrarectally injecting *N*-nitroso-*N*-methylurethane in BALB/c mice.<sup>30</sup> CT26 cells stably expressing human cancer/testis antigen MAGE-A4 (CT26/MAGE-A4) were established as described previously.<sup>21</sup> CMS5a is a subclone derived from CMS5, a 3-methylcholanthrene-induced sarcoma cell line of BALB/c origin, and expresses mERK2 as a neoantigen.<sup>20</sup> In *in vivo* tumor growth experiments, mice ( $n = 4$  or more) were inoculated subcutaneously in the right hind flank with 10<sup>6</sup> CT26/MAGE-A4 or CMS5a cells and monitored three times a week. The tumor size was estimated using the following formula: tumor size (mm<sup>3</sup>) = 1/2[length (mm) × width (mm)<sup>2</sup>].

**Tracking of the Subcutaneously Injected CHP or CHP:LPA Complex.** For tracking of the injected CHP nanogel, rhodamine-labeled CHP nanogel was subcutaneously injected to the back of BALB/c mice. Six hours later, the skin harboring DLN was harvested and observed using confocal laser scanning microscope (LSM780, Carl Zeiss, Germany). For tracking of the injected CHP:LPA, a fluorescently labeled LPA complexed with the CHP nanogel was subcutaneously injected into the right hind flank of the mice. The inguinal DLN was harvested 16 h after the injection, mashed, and filtered through a nylon mesh. The resulting cell suspension was analyzed using flow cytometry for incorporation of labeled LPA and expression of CD11b, CD11c, CD169, F4/80, CD3 $\epsilon$ , and B220. For immunohistochemical analysis, cryosections were prepared from the DLN. Optimum cutting temperature (O.C.T.) compound-embedded cryosections were stained with fluorescent dye-conjugated anti-CD169 or anti-F4/80 monoclonal antibodies (mAbs) and examined under a fluorescence microscope (BX53F, Olympus).

**Immunization of Mice.** The CHP:LPA complex or LPA emulsified with IFA (Sigma-Aldrich) was subcutaneously injected into the back of mice at the dose of 50  $\mu$ g as LPA. Phosphorothioate-containing CpG ODN 1668 (Hokkaido System Science, Japan) or poly-ICLC RNA (Oncovir, Inc.) was simultaneously and subcutaneously injected near the site of vaccination. To deplete macrophages, a clodronate liposome solution (FormuMax Scientific) was subcutaneously injected into the footpad of mice 6 days prior to immunization.

**Flow Cytometric Analysis.** Fluorescent dye-conjugated mAbs including anti-CD8 (53–6.7), anti-CD4 (RM4–5), anti-interferon (IFN)- $\gamma$  (XMG1.2), anti-CD80 (2D10.4), anti-CD86 (IT2.2), anti-CD11b (M1/70), anti-CD11c (N418), anti-F4/80 (BM8), anti-CD3 $\epsilon$  (145–2C11), anti-CD45R/B220 (RA3–6B2), and anti-CD169 (3D6.112) were purchased from Biolegend. The cell suspension prepared from the inguinal DLN or spleen was stained for surface markers using antibodies at the appropriate concentrations in PBS containing 2% fetal bovine serum for 15 min at 4 °C, and analyzed on a FACSCanto II system (BD Biosciences). For intracellular cytokine staining, splenocytes were incubated with mERK2 LPA or MAGE-A4 LPA for 1 h at 37 °C and then incubated for an additional 6 h with GolgiPlug (BD Bioscience). After permeabilization and fixation using the



Cytofix/Cytoperm Kit (BD Bioscience), the cells were stained with allophycocyanin-conjugated anti-IFN- $\gamma$  mAb and analyzed using flow cytometry.

**T Cell Proliferation and IFN- $\gamma$  Release Assay.** For *in vitro* T cell proliferation assay, the CHP:mERK2 LPA and CpG ODN were subcutaneously injected into the footpad of mice. DLN was resected 20 h after the injection. To isolate CD11b<sup>+</sup> cells, the total cell suspension prepared from the DLN was mixed with anti-CD11b microbeads (Miltenyi Biotec) and separated by positive selection on a magnetic bead column. For further fractionation of CD11b<sup>+</sup> cells, the cells were stained with FAM-labeled anti-CD11b, PE-labeled anti-CD169, PerCP-Cy5.5-labeled anti-F4/80, and allophycocyanin-labeled anti-CD11c mAbs, and sorted using a FACSAria system (BD Biosciences). The isolated cells (0.1, 0.3, or  $1 \times 10^5$ ) were then cocultured with  $2.5 \times 10^5$  DUC18 T cells prelabeled with carboxyfluorescein succinimidyl ester (CFSE) for 48 h. The dilution of CFSE was measured using flow cytometry to determine cell proliferation. IFN- $\gamma$  release into the culture medium at 48 h was quantified using a mouse IFN- $\gamma$  ELISA kit (BD Bioscience).

For *in vivo* T cell proliferation assay, either the CHP:mERK2 LPA or IFA:mERK2 LPA was subcutaneously injected into the back of mice. At day 0 or day 4,  $2.5 \times 10^5$  DUC18 T cells prelabeled with CFSE were intravenously infused into the vaccinated mice. DLNs were collected on day 3 or day 7, and dilution of CFSE was measured using flow cytometry to determine the *in vivo* proliferation of DUC18 T cells.

**In Vitro Cross-Presentation by Human Macrophages.** Peripheral blood mononuclear cells were isolated from buffy coats prepared using density gradient centrifugation of the blood of HLA-A0201-positive healthy donors over Ficoll. CD14<sup>+</sup> cells were purified with anti-CD14 microbeads and then incubated with GM-CSF, 20 ng/mL in the X-VIVO15 medium, for 7 days to induce differentiation to macrophages. The obtained macrophages were pulsed with human CHP:NMW LPA (10  $\mu$ g/mL) and stimulated with poly-I:LC RNA (10  $\mu$ g/mL). The human IFN- $\gamma$  enzyme-linked immunospot (ELISPOT) assay was performed as previously described. Briefly, a 96-well nitrocellulose ELISPOT plate (Millipore) was coated with an anti-human IFN- $\gamma$  mAb (clone 1-D1K, Mabtech) overnight at 4 °C. The wells were washed with PBS containing 0.01% Tween 20 (PBS-T) and blocked with the RPMI1640 medium containing 10% fetal calf serum for 2 h at 37 °C. HLA-A0201-restricted NY-ESO-1 epitope-specific CD8<sup>+</sup> T cells (clone 1G4,  $10^5$  cells per well) and antigen-pulsed macrophages were seeded into each well. After incubation for 22 h at 37 °C in 5% CO<sub>2</sub>, the plate was washed thoroughly with PBS-T. A biotin-conjugated anti-human IFN- $\gamma$  mAb (clone 7-B6-1, Mabtech) was then added (final concentration 1.25  $\mu$ g/mL), and the plate was incubated overnight at 4 °C. After a wash step with PBS-T, a streptavidin-alkaline phosphatase conjugate (1  $\mu$ g/mL; Roche Diagnostics) was added. After incubation for 60 min at room temperature, the wells were washed thrice with PBS-T and stained using an alkaline phosphatase conjugate substrate kit (Life Technologies). The reaction was stopped by intensive washing with distilled water. After the plate dried out, the number of spots in each well was counted using an ELISPOT reader (Cellular Technologies, Ltd.).

**Statistical Analysis.** The data were analyzed using Student's *t* test, Dunnett's multiple comparison test, or Tukey-Kramer multiple comparison test. Differences with *p* < 0.05 were considered statistically significant.

**Conflict of Interest:** The authors declare the following competing financial interest(s): Naozumi Harada is an employee of ImmunoFrontier, Inc. The other authors have no conflicts of interest.

**Acknowledgment.** We thank Drs. T. Kato and N. Seo for helpful discussion and Dr. L. Wang for technical assistance. This study was supported by a Grant-in-Aid for Scientific Research (KAKENHI) and the Exploratory Research for Advanced Technology (ERATO) research funding program.

**Supporting Information Available:** Characterization of the nanogel:LPA complex, associated *in vivo* mouse immunological data, and *in vitro* experiment with human macrophages. This material is available free of charge via the Internet at <http://pubs.acs.org>.

## REFERENCES AND NOTES

- Reddy, S. T.; van der Vlies, A. J.; Simeoni, E.; Angeli, V.; Randolph, G. J.; O'Neil, C. P.; Lee, L. K.; Swartz, M. A.; Hubbell, J. A. Exploiting Lymphatic Transport and Complement Activation in Nanoparticle Vaccines. *Nat. Biotechnol.* **2007**, *25*, 1159–1164.
- Kourtis, I. C.; Hirosue, S.; de Titta, A.; Kontos, S.; Stegmann, T.; Hubbell, J. A.; Swartz, M. A. Peripherally Administered Nanoparticles Target Monocytic Myeloid Cells, Secondary Lymphoid Organs and Tumors in Mice. *PLoS One* **2013**, *8*, e61646.
- Kobiyama, K.; Aoshi, T.; Narita, H.; Kuroda, E.; Hayashi, M.; Tetsutani, K.; Koyama, S.; Mochizuki, S.; Sakurai, K.; Katakai, Y.; *et al.* Nonagonistic Dectin-1 Ligand Transforms CpG into a Multitask Nanoparticulate TLR9 Agonist. *Proc. Natl. Acad. Sci. U.S.A.* **2014**, *111*, 3086–3091.
- Li, A. V.; Moon, J. J.; Abraham, W.; Suh, H.; Elkhader, J.; Seidman, M. A.; Yen, M.; Im, E. J.; Foley, M. H.; Barouch, D. H.; *et al.* Generation of Effector Memory T Cell-Based Mucosal and Systemic Immunity with Pulmonary Nanoparticle Vaccination. *Sci. Transl. Med.* **2013**, *5*, 204–130.
- Schlosser, E.; Mueller, M.; Fischer, S.; Basta, S.; Busch, D. H.; Gander, B.; Groettrup, M. TLR Ligands and Antigen Need to Be Coencapsulated into the Same Biodegradable Microsphere for the Generation of Potent Cytotoxic T Lymphocyte Responses. *Vaccine* **2008**, *26*, 1626–1637.
- Trombetta, E. S.; Mellman, I. Cell Biology of Antigen Processing *in Vitro* and *in Vivo*. *Annu. Rev. Immunol.* **2005**, *23*, 975–1028.
- Asano, K.; Nabeyama, A.; Miyake, Y.; Qiu, C. H.; Kurita, A.; Tomura, M.; Kanagawa, O.; Fujii, S.; Tanaka, M. CD169-Positive Macrophages Dominate Antitumor Immunity by Crosspresenting Dead Cell-Associated Antigens. *Immunity* **2011**, *34*, 85–95.
- Schliehe, C.; Redaelli, C.; Engelhardt, S.; Fehlings, M.; Mueller, M.; van Rooijen, N.; Thiry, M.; Hildner, K.; Weller, H.; Groettrup, M. CD8<sup>+</sup> Dendritic Cells and Macrophages Cross-Present Poly(D,L-Lactate-co-Glycolate) Acid Microsphere-Encapsulated Antigen *in Vivo*. *J. Immunol.* **2011**, *187*, 2112–2121.
- Sasaki, Y.; Akiyoshi, K. Nanogel Engineering for New Nanobiomaterials: from Chaperoning Engineering to Biomedical Applications. *Chem. Rec.* **2010**, *10*, 366–376.
- Akiyoshi, K.; Deguchi, S.; Moriguchi, N.; Yamaguchi, S.; Sunamoto, J. Self-Aggregates of Hydrophobized Polysaccharides in Water. *Macromolecules* **1993**, *26*, 3062–3068.
- Akiyoshi, K.; Deguchi, S.; Tajima, T.; Nishikawa, T.; Sunamoto, J. Microscopic Structure and Thermoresponsiveness of a Hydrogel Nanoparticle by Self-Assembly of a Hydrophobized Polysaccharide. *Macromolecules* **1997**, *30*, 857–861.
- Sasaki, Y.; Iida, D.; Takahashi, H.; Sawada, S.; Akiyoshi, K. Artificial Chaperone Polysaccharide Nanogels for Protein Delivery: a Thermodynamic Study of Protein-Nanogel Interactions Using Fluorescence Correlation Spectroscopy. *Curr. Drug Discovery Technol.* **2011**, *8*, 308–313.
- Shimizu, T.; Kishida, T.; Hasegawa, U.; Ueda, Y.; Imanishi, J.; Yamagishi, H.; Akiyoshi, K.; Otsuji, E.; Mazda, O. Nanogel DDS Enables Sustained Release of IL-12 for Tumor Immunotherapy. *Biochem. Biophys. Res. Commun.* **2008**, *367*, 330–335.
- Alles, N.; Soysa, N. S.; Hussain, M. D.; Tomomatsu, N.; Saito, H.; Baron, R.; Morimoto, N.; Aoki, K.; Akiyoshi, K.; Ohya, K. Polysaccharide Nanogel Delivery of a TNF- $\alpha$  and RANKL Antagonist Peptide Allows Systemic Prevention of Bone Loss. *Eur. J. Pharm. Sci.* **2009**, *37*, 83–88.
- Ikuta, Y.; Katayama, N.; Wang, L.; Okugawa, T.; Takahashi, Y.; Schmitt, M.; Gu, X.; Watanabe, M.; Akiyoshi, K.; Nakamura, H.; *et al.* Presentation of a Major Histocompatibility Complex Class 1-Binding Peptide by Monocyte-Derived Dendritic Cells Incorporating Hydrophobized Polysaccharide-Truncated HER2 Protein Complex: Implications for a Polyvalent Immuno-Cell Therapy. *Blood* **2002**, *99*, 3717–3724.
- Hasegawa, K.; Noguchi, Y.; Koizumi, F.; Uenaka, A.; Tanaka, M.; Shimono, M.; Nakamura, H.; Shiku, H.; Gnjatic, S.; Murphy, R.; *et al.* *In Vitro* Stimulation of CD8 and CD4 T

- Cells by Dendritic Cells Loaded with a Complex of Cholesterol-Bearing Hydrophobized Pullulan and NY-ESO-1 Protein: Identification of a New HLA-DR15-Binding CD4 T-Cell Epitope. *Clin. Cancer Res.* **2006**, *12*, 1921–1927.
17. Kageyama, S.; Wada, H.; Muro, K.; Niwa, Y.; Ueda, S.; Miyata, H.; Takiguchi, S.; Sugino, S. H.; Miyahara, Y.; Ikeda, H.; *et al.* Dose-Dependent Effects of NY-ESO-1 Protein Vaccine Complexed with Cholesteryl Pullulan (CHP-NY-ESO-1) on Immune Responses and Survival Benefits of Esophageal Cancer Patients. *J. Transl. Med.* **2013**, *11*, 246–255.
  18. Kaneo, Y.; Tanaka, T.; Nakano, T.; Yamaguchi, Y. Evidence for Receptor-Mediated Hepatic Uptake of Pullulan in Rats. *J. Controlled Release* **2001**, *70*, 365–373.
  19. Coulstock, E.; Sosabowski, J.; Ovečka, M.; Prince, R.; Goodall, L.; Mudd, C.; Sepp, A.; Davies, M.; Foster, J.; Burnet, J.; *et al.* Liver-Targeting of Interferon-Alpha with Tissue-Specific Domain Antibodies. *PLoS One* **2013**, *8*, e57263.
  20. Ikeda, H.; Ohta, N.; Furukawa, K.; Miyazaki, H.; Wang, L.; Kuribayashi, K.; Old, L. J.; Shiku, H. Mutated Mitogen-Activated Protein Kinase: a Tumor Rejection Antigen of Mouse Sarcoma. *Proc. Natl. Acad. Sci. U.S.A.* **1997**, *94*, 6375–6379.
  21. Muraoka, D.; Nishikawa, H.; Noguchi, T.; Wang, L.; Harada, N.; Sato, E.; Luescher, I.; Nakayama, E.; Kato, T.; Shiku, H. Establishment of Animal Models to Analyze the Kinetics and Distribution of Human Tumor Antigen-Specific CD8<sup>+</sup> T Cells. *Vaccine* **2013**, *31*, 2110–2118.
  22. Gray, E. E.; Cyster, J. G. Lymph Node Macrophages. *J. Innate Immun.* **2012**, *4*, 424–436.
  23. Coffman, R. L.; Sher, A.; Seder, R. A. Vaccine Adjuvants: Putting Innate Immunity to Work. *Immunity* **2010**, *33*, 492–503.
  24. Huang, X.; Yang, Y. Targeting the TLR9-MyD88 Pathway in the Regulation of Adaptive Immune Responses. *Expert Opin. Ther. Targets* **2010**, *14*, 787–796.
  25. Hanson, H. L.; Donermeyer, D. L.; Ikeda, H.; White, J. M.; Shankaran, V.; Old, L. J.; Shiku, H.; Schreiber, R. D.; Allen, P. M. Eradication of Established Tumors by CD8<sup>+</sup> T Cell Adoptive Immunotherapy. *Immunity* **2000**, *13*, 265–276.
  26. Barral, P.; Polzella, P.; Bruckbauer, A.; van Rooijen, N.; Besra, G. S.; Cerundolo, V.; Batista, F. D. CD169<sup>+</sup> Macrophages Present Lipid Antigens to Mediate Early Activation of iNKT Cells in Lymph Nodes. *Nat. Immunol.* **2010**, *11*, 303–312.
  27. Hailemichael, Y.; Dai, Z.; Jaffarizad, N.; Ye, Y.; Medina, M. A.; Huang, X. F.; Dorta-Estremera, S. M.; Greeley, N. R.; Nitti, G.; Peng, W.; *et al.* Persistent Antigen at Vaccination Sites Induces Tumor-Specific CD8<sup>+</sup> T Cell Sequestration, Dysfunction and Deletion. *Nat. Med.* **2013**, *19*, 465–472.
  28. DeLeo, A. B.; Shiku, H.; Takahashi, T.; John, M.; Old, L. J. Cell Surface Antigens of Chemically Induced Sarcomas of the Mouse. I. Murine Leukemia Virus-Related Antigens and Alloantigens on Cultured Fibroblasts and Sarcoma Cells: Description of a Unique Antigen on BALB/c Meth A Sarcoma. *J. Exp. Med.* **1997**, *146*, 720–734.
  29. Muraoka, D.; Kato, T.; Wang, L.; Maeda, Y.; Noguchi, T.; Harada, N.; Takeda, K.; Yagita, H.; Guillaume, P.; Luescher, I.; *et al.* Peptide Vaccine Induces Enhanced Tumor Growth Associated with Apoptosis Induction in CD8<sup>+</sup> T Cells. *J. Immunol.* **2010**, *185*, 3768–3776.
  30. Griswold, D. P.; Corbett, T. H. A Colon Tumor Model for Anticancer Agent Evaluation. *Cancer* **1975**, *36*, 2441–2444.
  31. Getts, D. R.; Martin, A. J.; McCarthy, D. P.; Terry, R. L.; Hunter, Z. N.; Yap, W. T.; Getts, M. T.; Pleiss, M.; Luo, X.; King, N. J.; *et al.* Microparticles Bearing Encephalitogenic Peptides Induce T-Cell Tolerance and Ameliorate Experimental Autoimmune Encephalomyelitis. *Nat. Biotechnol.* **2012**, *30*, 1217–1224.
  32. Backer, R.; Schwandt, T.; Greuter, M.; Oosting, M.; Jüngerkes, F.; Tüting, T.; Boon, L.; O'Toole, T.; Kraal, G.; Limmer, A.; *et al.* Effective Collaboration Between Marginal Metallophilic Macrophages and CD8<sup>+</sup> Dendritic Cells in the Generation of Cytotoxic T Cells. *Proc. Natl. Acad. Sci. U.S.A.* **2010**, *107*, 216–221.
  33. Blander, J. M. Phagocytosis and Antigen Presentation: a Partnership Initiated by Toll-Like Receptors. *Ann. Rheum. Dis.* **2008**, *67*, iii44–49.
  34. Segura, E.; Durand, M.; Amigorena, S. Similar Antigen Cross-Presentation Capacity and Phagocytic Functions in All Freshly Isolated Human Lymphoid Organ-Resident Dendritic Cells. *J. Exp. Med.* **2013**, *210*, 1035–1047.
  35. Akiyoshi, K.; Kobayashi, S.; Shichibe, S.; Mix, D.; Baudys, M.; Kim, S. W.; Sunamoto, J. Self-Assembled Hydrogel Nanoparticle of Cholesterol-Bearing Pullulan as a Carrier of Protein Drugs: Complexation and Stabilization of Insulin. *J. Controlled Release* **1998**, *54*, 313–320.
  36. Ayame, H.; Morimoto, N.; Akiyoshi, K. Self-Assembled Cationic Nanogels for Intracellular Protein Delivery System. *Bioconjugate Chem.* **2008**, *19*, 882–890.
  37. Takeda, S.; Takahashi, H.; Sawada, S.; Sasaki, S.; Akiyoshi, K. Amphiphilic Nanogel of Enzymatically Synthesized Glycogen as an Artificial Molecular Chaperone for Effective Protein Refolding. *RSC Adv.* **2013**, *3*, 25716–25718.